IIETA International Information and Engineering Technology Association
Advancing the World of Information and Engineering

Traitement du Signal
Vol. 42, No. 4, August, 2025, pp. 2107-2118
Journal homepage: http://iieta.org/journals/ts

Delivery Type (Induced or Cesarean) Classification with Deep Learning Method Using Shannon Entropy of Electrohysterogram Signal

Hamed Shamsi[1*], Sayyad Alizadeh[2]

[1] Faculty of Engineering, Department of Metallurgical and Materials Engineering, Karadeniz Technical University, Trabzon 61080, Turkey
[2] Department of Software Development, Karadeniz Technical University, Trabzon 61080, Turkey

Corresponding Author Email: Hshamsi@ktu.edu.tr

https://doi.org/10.18280/ts.420423

Received: 8 March 2025
Revised: 9 May 2025
Accepted: 11 June 2025
Available online: 14 August 2025

Keywords:
electrohysterogram (EHG), Shannon Entropy, induced, cesarean, LSTM

ABSTRACT

Current methods in the literature for predicting preterm birth using electrohysterogram (EHG) signals generally concentrate only on classifying term and preterm spontaneous deliveries. However, a realistic approach should also include other delivery types, such as induced, cesarean, and induced-cesarean sections. We can increase the precision of labor stage identification and better understand preterm birth risk by examining the characteristics of EHG signals unique to various delivery methods. In this study, the methodology involves preprocessing EHG signals and extracting key features through Shannon Entropy and logarithmic energy. These features, which do not need complicated models, are effective in highlighting the key traits and complexity of the signals. Thanks to their high sensitivity, they can identify even the most subtle shifts in uterine activity. The adaptive synthetic (ADASYN) oversampling technique is applied after extracting features to address the class imbalance. These features are then examined using three machine learning models: Random Forest (RF), Support Vector Machine (SVM), and Long Short-Term Memory (LSTM) to evaluate their effectiveness in distinguishing different types of delivery. The ICEHG-DS database was used to evaluate the performance of the proposed method, and the best results were achieved for the LSTM method using the Shannon Entropy feature extracted from channel S3, yielding an average F1-score of 99.34% and an accuracy of 99.33%. This work demonstrates the feasibility of accurately predicting the type of delivery by analyzing EHG signals as early as the 23rd week of pregnancy, utilizing a feature extraction method with low computational complexity.

1. INTRODUCTION

According to the World Health Organization (WHO) 2019 report, around 14 million pregnant women suffered preterm delivery, accounting for about 10% of all deliveries in that year. According to the organization's statistics, complications from premature birth claimed the lives of about 900,000 babies. Therefore, one of the most important challenges in global health is determining what causes preterm birth and creating ways to anticipate it weeks or even months in advance [1]. Various factors, including medically necessary or induced amniotic sac ruptures before 37 weeks and other underlying health issues, can lead to the early onset of labor [2]. Preterm birth can be triggered by several health conditions, such as infections, inflammation of the uterus, ruptured blood vessels, poor uterine blood circulation, and intense uterine contractions. A higher risk of premature birth can also be caused by risk factors such as high blood pressure, diabetes, prior cervical surgeries (like conization), uterine abnormalities, unhealthy lifestyle choices like smoking, drinking, or using drugs, and poor general health [3, 4].

Accurately predicting preterm birth continues to be a major challenge, even with significant research. However, examining uterine electrohysterogram (EHG) offers a hopeful path to enhancing the precision of predictions. This approach, which can be performed fully or semi-automatically using low-cost methods [5-10], can enable the prediction of weeks or even months in advance of preterm birth. Uterine contractions, which are vital for labor, are caused by swift electrical signals within the uterine muscles [11]. EHG signals capture variations in the electrical potential of the uterus, allowing for a precise and non-invasive assessment of its function [12]. According to a review of current research, EHG signals provide more detailed information for predicting labor, achieving higher accuracy than other existing methods [7]. There are two primary strategies for predicting preterm birth with EHG signals: examining data from both the pre-labor and labor phases, and comparing pregnancies that occurred before and after 37 weeks [8-10, 13]. Conventional methods usually center around analyzing contraction intervals, but this approach restricts the data, particularly in early pregnancy when contractions are rare.

Accurately predicting preterm birth and delivery outcomes remains a critical challenge in obstetrics, with significant implications for maternal and fetal health. EHG signals, which capture uterine electrical activity, offer a promising non-

invasive approach for early prediction [7, 9]. Evidence suggests that analyzing both contraction and non-contraction (dummy) intervals in EHG records can enhance classification accuracy without requiring prior annotation of contractions [9]. Various signal processing methods have been explored to extract linear and nonlinear features, including time-domain characteristics, frequency-domain properties, and complexity metrics, to classify EHG records for preterm and term deliveries [9, 10, 14-26]. However, existing methods predominantly focus on distinguishing spontaneous preterm and term deliveries, often neglecting other delivery types such as induced, cesarean, and induced-cesarean sections, particularly in early pregnancy stages.

The rising global rates of induced and cesarean deliveries, which account for significant maternal and fetal health risks, underscore the need for comprehensive prediction models that include these delivery types [27, 28]. Induced labor, often necessitated by conditions like preeclampsia or fetal distress, can lead to prolonged labor and an increased likelihood of cesarean section, which is associated with higher maternal morbidity, including infection and hemorrhage, and complications in subsequent pregnancies [2]. Early identification of delivery type as early as the 23rd week of pregnancy can guide clinical decision-making, enabling obstetricians to optimize induction protocols, reduce unnecessary cesarean sections, and improve maternal-fetal outcomes. Current EHG-based methods, however, primarily rely on late-stage signals (after 37 weeks) and focus on spontaneous labor, leaving a critical gap in early prediction for diverse delivery types [29, 30]. This study addresses this gap by proposing a novel method to classify induced, cesarean, and induced-cesarean deliveries using EHG signals from the 23rd week of pregnancy. By leveraging simple yet effective features (Shannon Entropy and Logarithmic Energy), our approach achieves high accuracy with low computational complexity, offering a robust tool for personalized obstetric care and improved health outcomes.

The TPEHG DB database, which was made public in 2011, includes 300 spontaneous EHG records from preterm and term pregnancies that were taken at various times (about 23 and 31 weeks). This database has enabled detailed research into nonlinear signal processing techniques and machine and deep learning methods to accurately predict preterm birth and classify pregnancies before and after 37 weeks [29]. A major limitation of this database is the class imbalance between preterm and term datasets (38 preterm vs. 262 term records).

The TPEHGT DS database (collected around the 31st week) is also frequently used in preterm birth prediction work. This dataset contains 13 recordings that include preterm and term pregnancies and measure uterine contractions. In this dataset, uterine contraction interval measurement is essential for differentiating between preterm and term deliveries. Data imbalance is the main challenge in biomedical databases, including TPEHG or ICEHG DS, where observations in one class (such as preterm births or cesarean deliveries) are substantially less numerous compared to the other [24, 31]. The performance of machine learning models may suffer as a result of this imbalance. Artificial generation of data methods like SMOTE or ADASYN are commonly utilized to address this issue, however, they have drawbacks as well [22, 32-34].

2. RELATED WORK

Identifying preterm and term births using various features, methods, and classifiers is the subject of numerous studies in the literature. The TPEHG and TPEHGT datasets are the main sources of data used in the investigations.

Fergus et al. [35] used a polynomial classifier as their detection approach with a feature set that included RMS, peak and median frequencies, sampleEn, and clinical data. To address data imbalance, the SMOTE oversampling technique was applied, and an average sensitivity of 96%, specificity of 90%, and overall accuracy of 95% are reported. Hussain et al. [36] used a Dynamic Neural Network as their detection technique and reported 89% sensitivity, 91% specificity, and 90% accuracy. These results were achieved using SMOTE oversampling and features similar to those used by Fergus et al. [35]. Smrdel and Jager [37] used a statistical classification technique named Quadratic Discriminant Analysis and SVM classifiers to detect term and preterm cases. The authors first filtered the EHG signal within a 0.3-4 Hz frequency range and then estimated smapelEn and median frequency from one of the EHG signal channels using the adaptive autoregressive method. After balancing the data with SMOTE, they reported 86% and 87% accuracy for each class, respectively.

Ren et al. [38] used empirical Mode Decomposition (EMD) to decompose the signals into their constituent Intrinsic Mode Functions (IMFs) and based on the instantaneous amplitude and frequency, the author extracts entropy ratios of these instantaneous as feature vectors. After applying the Min/Max technique for addressing data imbalance, the highest results were obtained using the Ada boost classifier with an AUC of 98/6%. Also, Fergus et al. [39] utilized extracted features from both the time and frequency domain of the EHG signals from the TPEHG database, along with the SMOTE oversampling technique for data balancing. The authors reported a sensitivity of 91%, specificity of 84%, and an AUC of 94%, achieved through a combination of advanced artificial neural network classifiers. Acharya et al. [22] employed to extract features from both the time and frequency domain based on EMD and Wavelet packet decomposition technique from 326 EHG recordings. After employing ADASYN to balance the database and SVM for classification, a sensitivity of 96.25%, specificity of 95.08%, accuracy of 97.33%, and AUC of 96.2% was achieved.

Ahmed et al. [32] extracted multivariate multiscale entropy from TPEHG signals and applied the ADASYN technique to balance the dataset. The best classification performance using an SVM, with a sensitivity of 92%, specificity of 98%, accuracy of 94.9%, and an AUC of 99% was reported. Degbedzui and Yüksel [33] extract a new feature by analyzing the frequency components of the EHG signal. The authors use the ADASYN technique to balance the data, and the best results achieved with the SVM method were an accuracy of 99.74%, specificity of 99.94%, and sensitivity of 99.55%.

Mischi et al. [31] extract new entropy measures for analyzing contraction data. The authors showed that these measures help quantify the complexity and regularity of the EHG signals, providing valuable features for distinguishing between term and preterm births with an average sensitivity of 61%, specificity of 83%, and accuracy of 73%. The authors did not specify the technique used for data balancing, and the database employed was non-public. Jager et al. [9] used a balanced dataset of TPEHGT (Contractions/Non-contraction) records, consisting of 53 terms and 47 preterms. In this work, the characteristics, complexity, and frequency properties of the EHG signals are evaluated. The features used as a feature vector include sampleEn, median frequency of power

spectrum and peak amplitude of normalized power spectrum. After applying SMOTE for both classes and employing quadratic discriminant analysis, this method achieved an average sensitivity of 89% - 87%, specificity of 89% - 91%, and accuracy of 88.68% - 88.79% for each class, respectively.

Chen and Xu [40] utilized a Sparse Autoencoder (SAE)-based deep neural network (DNN) classifier to predict preterm birth using EHG signals. The sampleEn and wavelet entropy were extracted from both preterm and term recordings in the TPEHGT database, which is a balanced dataset containing 450 terms and 450 preterm samples. The best results achieved by this method were: a sensitivity of 98.2%, a specificity of 97.74%, and an accuracy of 97.9%. Saleem et al. [41] applied Granger causal analysis to analyze the contraction and dummy intervals of recorded EHG signals. The TPEHGT dataset used in this study consists of 94 terms and 106 preterms samples. The features extracted from the analysis were the coupling strength and directionality indices, which formed the feature vector for classification. The best results achieved by this method were: a sensitivity of 86%, specificity of 90%, and accuracy of 84%. Peng et al. [42] investigated the relevance of linear and nonlinear features extracted from different gestational weeks (before the 26th week of gestation) using a random forest (RF) classifier. After feature extraction and selecting 15 features, and using ADASYN to handle class imbalance, an accuracy of 93%, sensitivity of 89%, and specificity of 97% were reported.

Nieto-del-Amor et al. [43] proposed an ensemble classifier for term and preterm detection based on nonlinear, temporal, and spectral features extracted from EHG signals across different bandwidths and all recording channels. Feature selection was performed using a genetic algorithm. Following the SMOTE method, a mean F1 score of 92.04% was achieved. Later, in another study, Nieto-del-Amor et al. [44] used a linear discriminant analysis (LDA) classifier and entropy measures to classify term-preterm EHG recordings. The results demonstrated the effectiveness of this approach, with an average F1 score of 90.1% achieved.

Xu et al. [45] used a horizontal visibility graph (HVG) algorithm to extract features such as network degree density and distribution, clustering coefficient, and assortativity coefficient. These features were then used with an SVM classifier to predict preterm labor. To address data imbalance, they applied a partition-synthesis method. By employing this approach, they achieved an accuracy of 91%.

Researchers have developed various methods to distinguish between spontaneous labor at term (before the 41st week of gestation) and induced labor in late-term pregnancies [46]. These methods include characterizing EHG bursts in pregnant women with complete placenta previa using late antepartum EHG records, predicting the success of labor induction based on EHG measurements taken in the first hours after induction [47-49], using intrapartum cardiotocography traces to predict delivery modes such as cesarean section and spontaneous vaginal delivery [27], employing clinical attributes to forecast delivery modes [50], and monitoring uterine dynamics and predicting uterine atony after spontaneous vaginal or cesarean deliveries using postpartum EHG records [51]. However, the current methods for predicting delivery mode have been developed independently from the issue of preterm birth prediction and primarily rely on late antepartum or intrapartum records, all collected after the 37th week of pregnancy [28, 47, 48]. As a result, these methods are all focused on term pregnancies.

To our knowledge, there has been no research focused on the characterization and separation of uterine electromyography (EHG) records from induced labor and cesarean sections that were collected several weeks or even months before delivery. Such research is crucial to enhance our understanding of how key features evolve during pregnancy, as well as to predict the mode of delivery and evaluate the health conditions of both the mother and the baby at the time of delivery. This study aims to examine the physiological factors that may lead to induction, cesarean section, or a combination of both during pregnancy using the ICEHG DS dataset. The research seeks to determine whether early prediction of delivery methods, such as induced labor and cesarean section, is possible as early as the 23rd or 31st week of pregnancy by analyzing and classifying EHG records from the ICEHG DS.

3. MATERIALS AND METHODS

The main steps of the proposed method to classify the type of delivery (induced or cesarean) consists of four steps: (1) Data acquisition and preprocessing, (2) addressing the class imbalance problem using the Adaptive Synthetic (ADASYN) sampling approach, (3) feature extraction, and (4) detection of the type of delivery (induced or cesarean). The details of the proposed method are explained in the following subsections.

3.1 Data acquisition

In this paper, we utilize the Induced Cesarean Electrohysterogram Database (ICEHG DS), which is freely accessible on the Physionet website. This data was collected at the Clinical Department of Perinatology, University Medical Center Ljubljana, Ljubljana, Slovenia, from 1997 to 2006. This dataset has been ethically approved by the National Medical Ethics Committee of Slovenia (No. 32/01/97), with all data fully anonymized and informed consent obtained from all participants, as documented in the dataset publication [51]. EHG data are collected by placing four electrodes (E1, E2, E3, E4) on the abdominal surface of pregnant mothers (placement protocol, which is shown in Figure 1), Based on differences in electrical potentials between the electrodes, three channels were used for each recording: S1 = E2 − E1, S2 = E2 − E3, and S3 = E4 − E3. For each individual, recordings of approximately 30 minutes were digitized at a rate of 20 samples per second per channel, with a 16-bit resolution in a range of ± 2.5 millivolts. This data set was collected from 91 pregnant women. The available information regarding the number of mothers with Induced or Cesarean deliveries, as well as Induced-Cesarean deliveries and other necessary information, is provided in Table 1.

Table 1. The quantity of EHG records for each delivery type in the ICEHG DS database

Group	Delivery Group	Number of Subjects	Mean of Recording Time (Week)
Early	Cesarean	11	22.6
	Induced	38	22.9
	Induced-Cesarean	13	23.3
Late	Cesarean	8	30.8
	Induced	43	31.0
	Induced-Cesarean	13	31.2

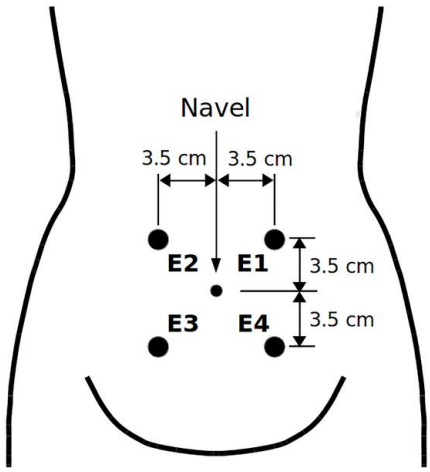

Figure 1. The electrode placement points for recording EHG signals [9]

3.2 Preprocessing

The signal recorded from the lower abdomen is a complex combination of the mother's electrocardiogram (MECG), the fetal electrocardiogram (FECG), and various other signals, including uterine activity (UA), myographic signals, and others [9]. To extract uterine activity signals, raw EHG data were processed using a fourth-order Butterworth band-pass filter. A double-pass filtering method was applied, with cut-off frequencies set at 0.08 Hz and 5 Hz. Given that most of the spectral content of the EHG signal falls within this frequency range, the focus of this study is on the EHG signals filtered using these specific cut-off frequencies. To reduce transient effects introduced by the filtering process, the initial and final 180 seconds of each recording were removed [51]. Figure 2 illustrates the raw EHG waveforms corresponding to the three delivery types induced, cesarean, and induced-cesarean, alongside their filtered counterparts.

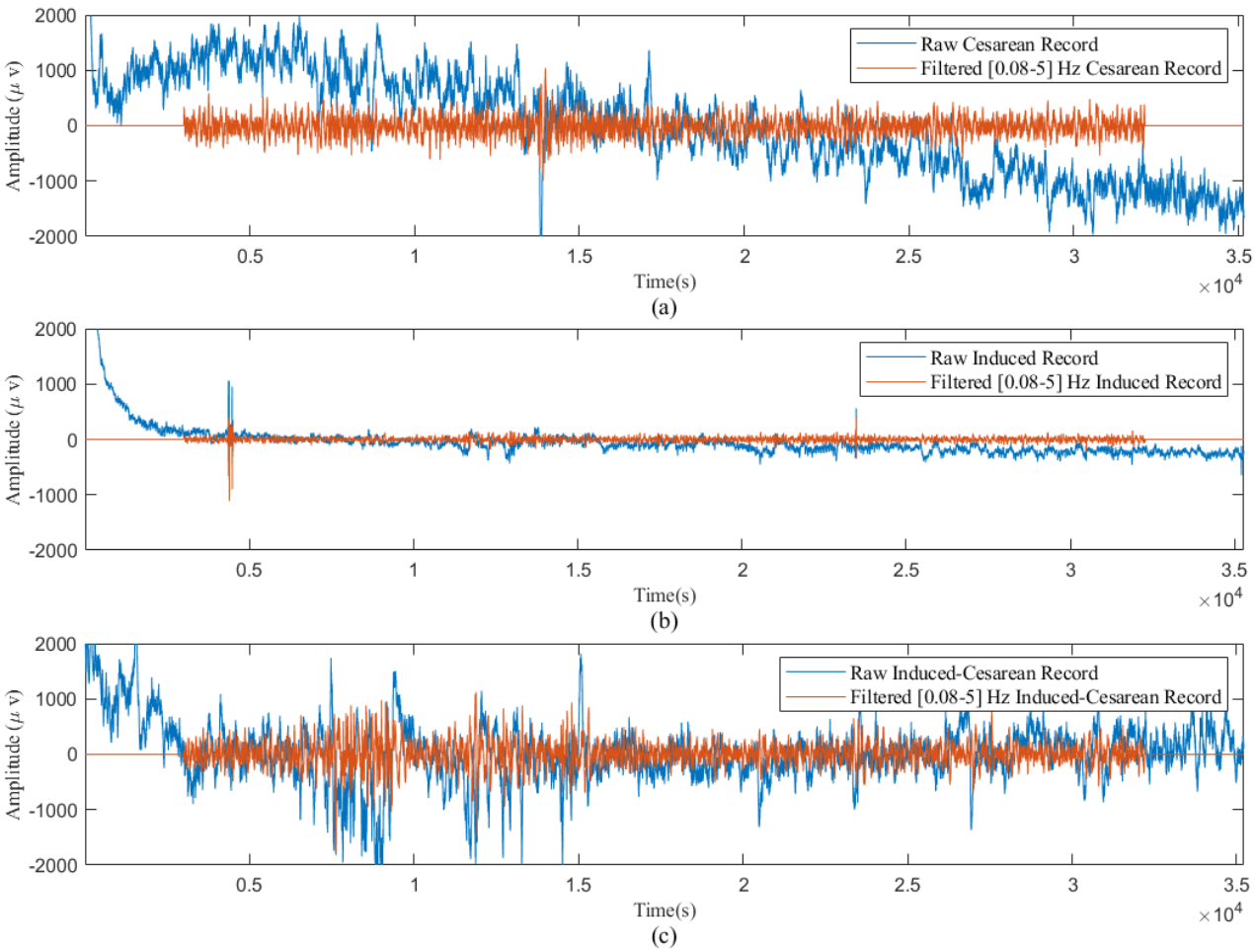

Figure 2. The raw EHG waveforms for the three delivery types, as well as their filtered versions: (a) Early Cesarean (b) Early Induced (c) Early Induced-Cesarean

3.3 Data balancing and normalization

The main issue with the ICEHG DS database is the imbalance in the distribution of data across the Cesarean, Induced, and Induced-Cesarean delivery classes. The original ICEHG DS consists of 19 Cesarean deliveries, 81 induced deliveries, and 43 late), and 26 induced-cesarean deliveries, with only 15% of the data corresponding to Cesarean deliveries and 20% to induced-cesarean deliveries, and 65% to induced deliveries. This imbalance can lead to classifiers being biased toward the induced deliveries. Given that classifiers are sensitive to detecting the majority class, it is crucial to balance the minority class. A common solution found in the literature is to generate synthetic samples for the underrepresented class using techniques such as SMOTE or ADASYN [52]. In this study, the ADASYN oversampling technique is used to address the data imbalance issue. Subsequently, all the data are rescaled to a fixed range of 0-1.

3.4 Feature extraction

EHG signals exhibit complex and dynamic patterns due to the intricate interactions of uterine cells, necessitating features that effectively capture their nonlinear and energy characteristics for accurate classification of delivery types. In the literature, various features have been explored for EHG analysis, including time-domain features (e.g., Root Mean Square, Mean Absolute Value), frequency-domain features (e.g., Median Frequency, Power Spectral Density), and nonlinear features (e.g., Sample and Dispersion Entropy) [9, 22, 31, 33]. In this study, we selected Shannon Entropy (Sh-En) and Logarithmic Energy (LogEn) as the primary features due to their simplicity, low computational complexity, and demonstrated effectiveness in modeling the complexity and energy dynamics of EHG signals [9, 15, 31].

Sh-En quantifies the uncertainty or randomness in the EHG signal, making it well-suited for capturing the irregular patterns associated with different delivery types. LogEn measures the signal's energy distribution across frames, which is particularly sensitive to the intensity of uterine contractions, hypothesized to be stronger in induced deliveries compared to cesarean or induced-cesarean cases. These features were chosen based on their theoretical alignment with the nonlinear and dynamic nature of EHG signals, as well as preliminary experiments with the ICEHG DS dataset that confirmed their suitability for distinguishing delivery types. Studies [38, 43] have utilized entropy-based measures to differentiate preterm and term EHG records, while the studies [9, 40] highlighted the effectiveness of simple features for classifying delivery groups (preterm, term, induced, cesarean), supporting our choice. Compared to time- and frequency-domain features (e.g., RMS, Median Frequency), Sh-En and LogEn offer superior performance in delivery type classification due to their lower sensitivity to noise, better ability to capture nonlinear EHG patterns, and reduced computational complexity, as evidenced by prior studies [9, 15, 28, 31, 38, 40, 43]. These characteristics make them more suitable for a cost-effective and robust classification system using the ICEHG DS dataset.

To prepare EHG signals for analysis, a band-pass filter (frequency range: 0.08 to 5 Hz) is applied to remove noise, such as power line interference and movement artifacts, preserving the relevant frequency components of uterine electrical activity. The filtered signal is then segmented into 3000-sample windows with a 1000-sample shift, and the Sh-En and LogEn of each frame are calculated. The equations for these features are defined as follows:

Shannon Entropy:

$$H_k = -\sum_{i=1}^{N} p_i \ln p_i \tag{1}$$

where, p_i represents the probability of the i-th value within the frame, and N represents the total number of frames analyzed for each EHG signal.

Logarithmic Energy:

$$z_k = ln\left(\frac{1}{N}\sum_{i=1}^{N} s(k,i)^2\right) \tag{2}$$

where, z_k denotes the logarithmic energy of the k-th frame, $s(k,i)$ represents the EHG signal within the frame, and N represents the total number of frames analyzed for each EHG signal. From each 29-minute EHG signal, 1448 frames were extracted for each delivery type (induced, cesarean, and induced-cesarean). The length of the extracted feature vector will be equal to the number of frames. The corresponding logarithmic energy and Shannon entropy are presented in Figure 3 for the different delivery types.

3.5 Delivery type classification

To implement the model, after feature extraction, we apply ADASYN to address the class imbalance. The balanced feature is then divided into training and testing sets: 80% for training and 20% for testing. The performance of the extracted features in distinguishing between Cesarean, Induced, and Induced-Cesarean classes is evaluated using three classifiers. To classify between induced, cesarean, and induced-cesarean deliveries, we use three classifiers: Long Short-Term Memory (LSTM), Support Vector Machine (SVM), and Random Forest (RF). These classifiers were selected because of their varying learning strategies, providing a well-rounded approach to the classification task. The decision to use these models is based on their established reliability and effectiveness in distinguishing between different delivery types, as supported by previous research and literature.

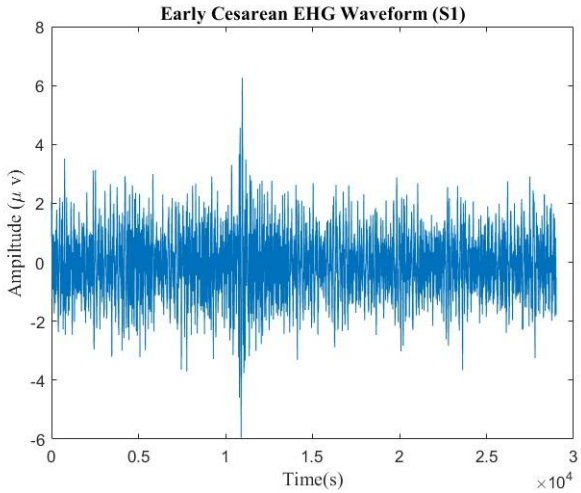

(a1)

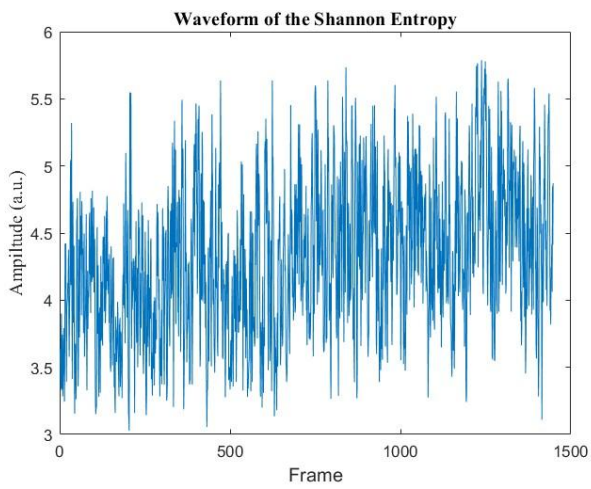

(a2)

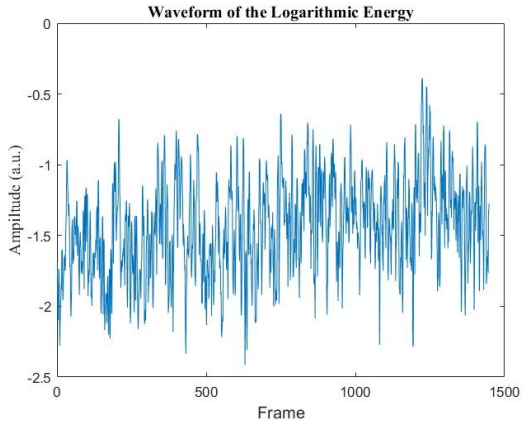

(a3)

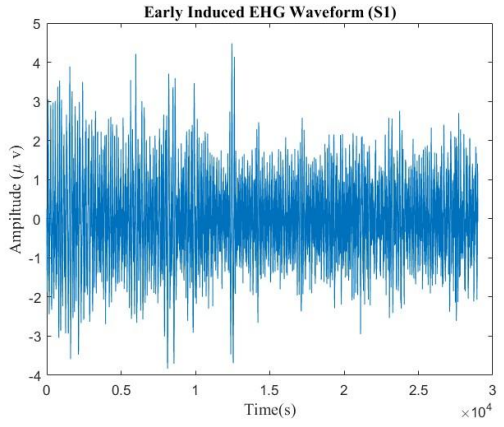

(b1)

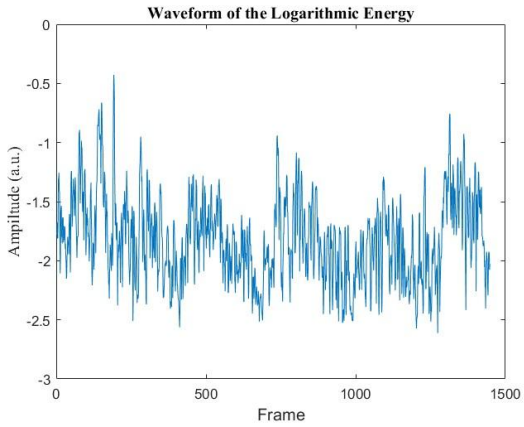

(b2)

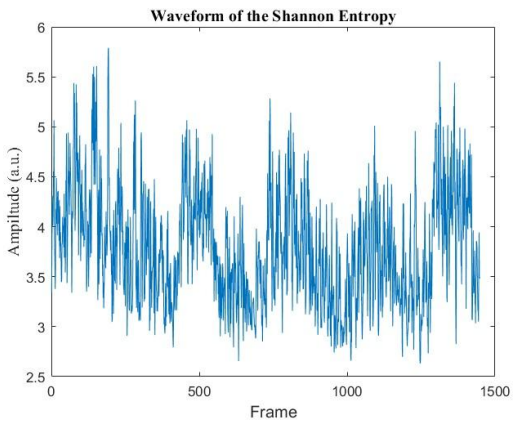

(b3)

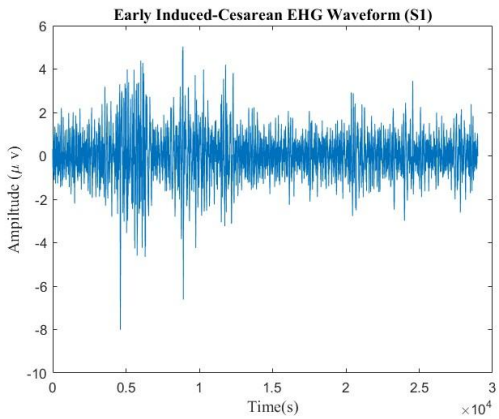

(c1)

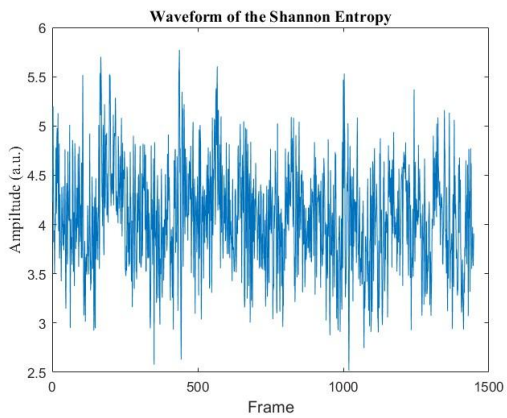

(c2)

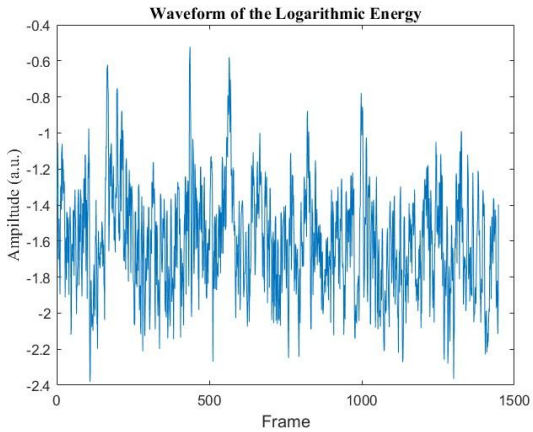

(c3)

Figure 3. The waveform of the EHG signal (channel S1) and the corresponding Sh-En and LogEn features are illustrated for three delivery types: Early Cesarean (a1, a2, a3), Early Induced (b1, b2, b3), and Early Induced-Cesarean (c1, c2, c3). Panels -1 show the EHG waveforms, panels -2 the Sh-En features, and panels -3 the LogEn features

3.6 Performance measures

The performance of the methods is evaluated using four quantitative metrics: True Positives (TP): Correctly predicted as the specific class (e.g., Induced, Cesarean, or Induced-Cesarean). True Negatives (TN): Correctly predicted as not belonging to the specific class. False Positives (FP): Incorrectly predicted as the specific class when it was not. False Negatives (FN): Incorrectly predicted as not belonging to the specific class when it should have. To evaluate the performance of the proposed classification algorithm, sensitivity (Se), specificity (Sp), accuracy (Acc), Precision (Pr), and F1 score are computed. The calculation rules of the metrics can be formulated as follows.

$$Se = \frac{TP}{TP + FN} \times 100 \tag{3}$$

$$Sp = \frac{TN}{TN + FP} \times 100 \tag{4}$$

$$Acc = \frac{TP + TN}{TP + TN + FN + FP} \times 100 \tag{5}$$

$$Pr = \frac{TP}{TP + FP} \times 100 \tag{6}$$

$$F1\ Score = 2 \times \frac{Pr \times Se}{Pr + Se} \tag{7}$$

4. RESULTS AND DISCUSSION

In this paper, to achieve better performance for each classifier, the experiments were repeated multiple times, and we report the best and most important parameters, with the remaining ones set to their default values. Based on a review of existing EHG signal classification methods, a series of experiments were performed to evaluate the effectiveness of the classification techniques used in this study. All experiments were conducted in MATLAB R2024a on a workstation equipped with three NVIDIA GeForce RTX 2080Ti GPUs (12 GB each).

4.1 Classification performance on ICEHG DS

Distribution plots for each delivery type in various entropy and log entropy measures are shown in Figure 4. The performance metrics for LSTM, SVM, and RF models, obtained through 10-fold cross-validation, are presented in Tables 2-4, respectively. In the initial stages of developing an SVM classification model, our preliminary analysis showed that the polynomial kernel models demonstrated superior performance compared to the linear kernel model, and the RBF model also produced similar results. Consequently, we decided to exclude the results of the linear kernel and RBF models from this report. Furthermore, we recognize the critical role of kernel parameters in effectively distinguishing between different birth types, such as cesarean and induced deliveries. To minimize classification errors, optimal kernel parameters are crucial. Therefore, we utilized MATLAB R2024a for its automatic tuning to maximize model performance.

The classification performance of the RF classifier using the extracted Shannon Entropy and logarithmic energy features is presented in Table 2. This table illustrates that Channel S3 achieved the highest classification performance with Sh-En features, recording an average 91.56 ± 0.0695 % accuracy. Channel S2 followed closely with an average accuracy of 90.67 ± 0.0631 %. Conversely, Channel S1 showed the lowest accuracy for Sh-En features, at 89.42 ± 0.1040%. With the same method, Channel S2 displayed the best performance for features extracted using LogEn with an average accuracy of 92.78 ± 0.0788%. In contrast, Channel S3 exhibited the lowest accuracy for LogEn features, at 90.56 ± 0.0456%.

Table 3 presents the classification accuracy results obtained using an SVM classifier. The analysis shows that the Shannon Entropy features extracted from Channel S3 exhibited the best performance, with a peak classification accuracy of 97.78 ± 0.0388%. Similarly, features extracted using logarithmic energy achieved the highest accuracy of 96.17 ± 0.0604% on Channel S1. On the other hand, the lowest accuracies were recorded on Channel S2, with Sh-En achieving 93.33% ± 0.0574% and LogEn reaching 94.44 ± 0.0586%.

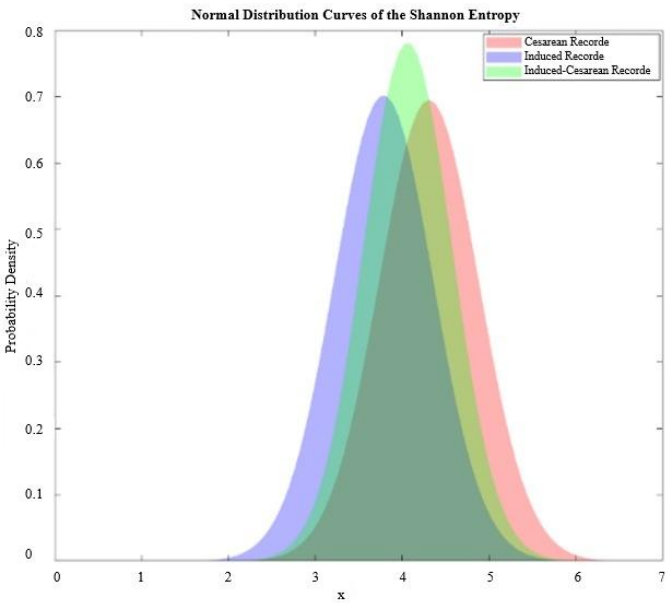

(a1)

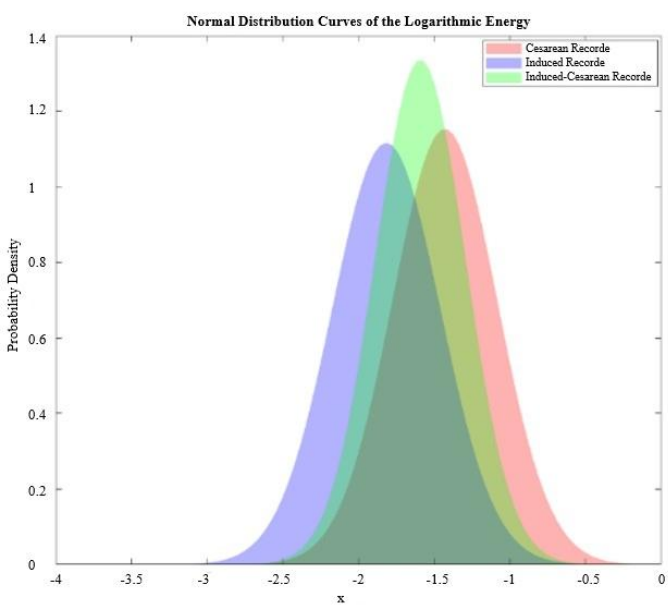

(a2)

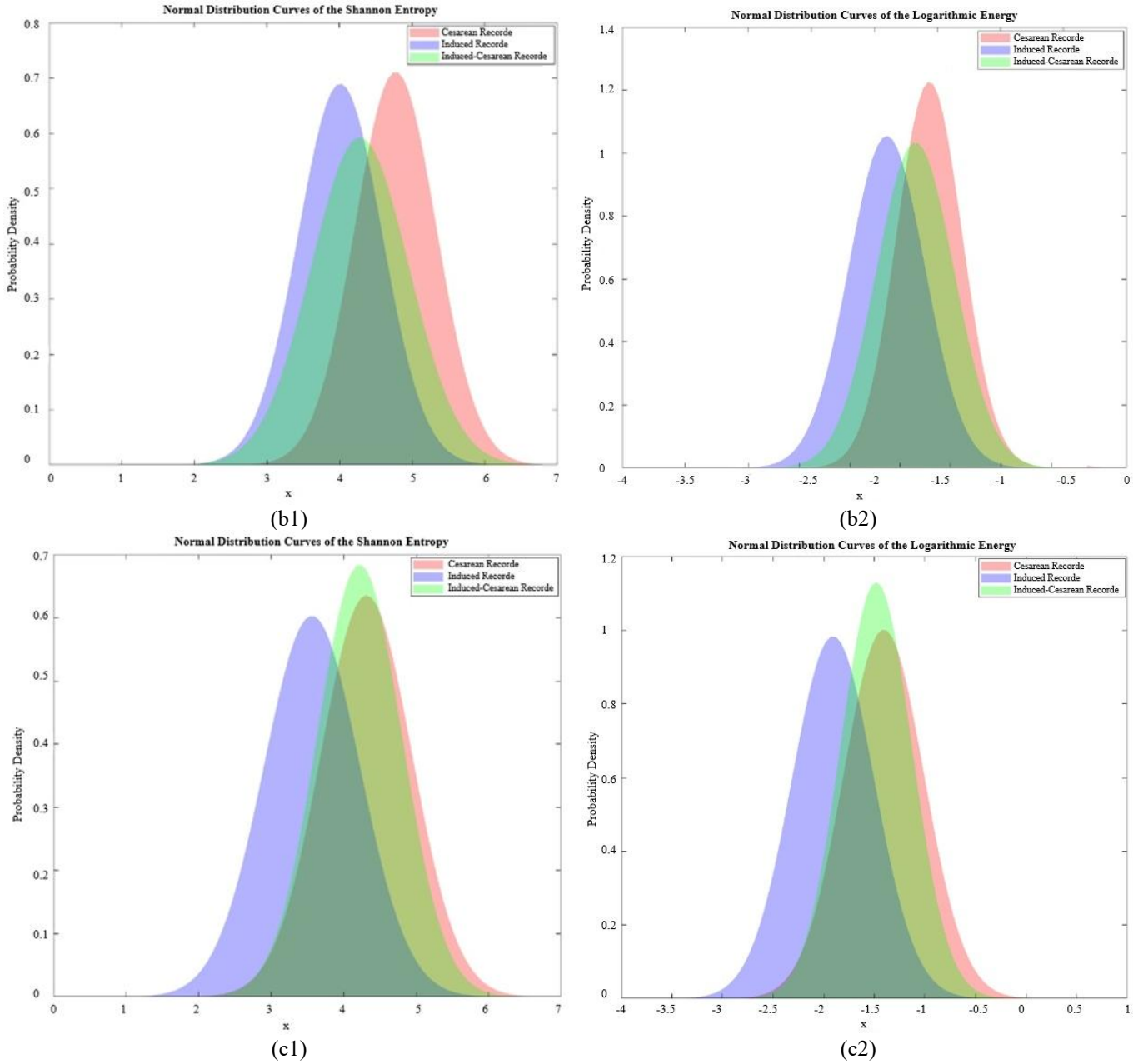

Figure 4. Distribution plots for various entropy and logarithmic measures: (a1), (b1), and (c1) display the normal Distribution of Sh-En for channels 1,2,3, respectively. (a2), (b2), and (c2) show the normal Distribution of LogEn for channels 1,2,3, respectively

Table 2. Performance of different channel configurations for various extracted features using the RF method

Feature	Channel	Se (%)	Sp (%)	ACC (%)
LogEn	CH1	94.40 ± 0.0927	90.46 ± 0.1262	90.73 ± 0.1061
	CH2	96.57 ± 0.0735	98.57 ± 0.0452	**92.78 ± 0.0788**
	CH3	94.89 ± 0.0858	92.13 ± 0.1164	90.56 ± 0.0456
Sh-En	CH1	94.40 ± 0.0939	89.88 ± 0.1824	89.42 ± 0.1040
	CH2	95.14 ± 0.1040	93.57 ± 0.1636	90.67 ± 0.0631
	CH3	98.00 ± 0.0689	92.25 ± 0.1010	**91.56 ± 0.0695**

Table 3. Performance of different channel configurations for various extracted features using the SVM method

Feature	Channel	Se (%)	Sp (%)	ACC (%)
LogEn	CH1	100.00 ± 0.0000	92.45 ± 0.0820	96.17 ± 0.0604
	CH2	100.00 ± 0.0000	92.82 ± 0.0983	94.44 ± 0.0586
	CH3	98.53 ± 0.0452	98.70 ± 0.0279	95.56 ± 0.0234
Sh-En	CH1	100.00 ± 0.0000	91.35 ± 0.1154	96.75 ± 0.0456
	CH2	99.67 ± 0.0.0298	94.17 ± 0.1245	93.33 ± 0.0574
	CH3	100.00 ± 0.0000	98.00 ± 0.0632	91.78 ± 0.0388

Table 4. Performance of different channel configurations for various extracted features using the LSTM method

Feature	Channel	Se (%)	Sp (%)	ACC (%)
LogEn	CH1	98.75 ± 0.0395	98.75 ± 0.0452	98.40 ± 0.0338
	CH2	96.05 ± 0.0672	97.13 ± 0.0612	96.76 ± 0.0448
	CH3	98.57 ± 0.0452	97.32 ± 0.0303	98.67 ± 0.0264
Sh-En	CH1	98.75 ± 0.0452	99.11 ± 0.0725	99.07 ± 0.0264
	CH2	94.64 ± 0.0941	99.76 ± 0.0124	96.67 ± 0.0606
	CH3	97.50 ± 0.0791	99.65 ± 0.0223	99.33 ± 0.0527

The classification results for the LSTM classifier are presented in Table 4. This table demonstrates that the extracted LogEn feature from channel S3 achieves the highest classification performance, with an average accuracy of 99.17 ± 0.0264 %. Channels S1 and S2 exhibit closely related performance, achieving average accuracies of 96.79 ± 0.0414% and 95.76 ± 0.0448%, respectively. Similarly, features extracted using Sh-En achieved the highest accuracy of 96.17 ± 0.0604% on Channel S3.

An analysis of Tables 2 to 4 in this article demonstrates that by extracting two key features from the structure of EHG signals, it becomes possible to effectively and accurately distinguish between Cesarean and Induced births.

Furthermore, the results indicate that all three channels yielded fairly acceptable outcomes in detecting various delivery records. Consequently, by utilizing the introduced features and employing a single measurement channel, the progress of labor and, subsequently, the mode of delivery can be effectively monitored. This approach offers cost-effectiveness and low computational demands.

4.2 Discussion of results and limitations

Table 5 presents the comparative performance F1-score measure of various classification models on the given dataset. Analyzing Tables 2 to 4 reveals that Channel S3 provided more acceptable results. This table demonstrates that the extracted LogEn feature from Channel S3 achieves the highest classification performance using the LSTM method, with an average F1-score of 99.15 ± 0.0275%. The SVM method exhibits closely related performance, reaching an average F1-score of 98.89 ± 0.0351%. Similarly, features extracted using Sh-En using the LSTM method achieved the highest accuracy of 99.34 ± 0.0186% on Channel S3. SVM method using the same feature, followed closely with an average accuracy of 99.21% ± 0.0263%.

Table 5. F1 score performance of different classification methods for extracted features in channel S3

Feature	RF	SVM	LSTM
LogEn	94.45 ± 0.0534	98.89 ± 0.0351	99.15 ± 0.0278
Sh-En	95.40 ± 0.0528	99.21 ± 0.0263	99.34 ± 0.0186

To address class imbalance in the ICEHG DS dataset, where minority classes (e.g., induced deliveries) were underrepresented, the Adaptive Synthetic Sampling (ADASYN) technique was used to generate synthetic samples. This improved the F1-score for the LSTM classifier with Shannon Entropy on Channel S3 from 82% (without ADASYN) to 99.34%, with real induced delivery samples achieving an F1-score of 95% [52]. To mitigate overfitting and noise, synthetic samples were used only during training, with real data reserved for testing, and 10-fold cross-validation ensured model generalization [53]. ADASYN's parameters (e.g., number of nearest neighbours) were tuned to minimize distribution shifts, verified using Kullback-Leibler divergence to align synthetic and real data distributions [53]. However, reliance on synthetic data may not fully capture real-world EHG variability, a limitation we aim to address by collecting larger real-world datasets and exploring alternatives like SMOTE or cost-sensitive learning.

Despite the high performance, EHG-based predictions of delivery types (induced or cesarean) lack full interpretability, limiting their use for definitive medical decisions without additional clinical tests [38]. These predictions, representing probabilities, require further development for reliable hospital use [43]. Patient data privacy, addressed through anonymization in the ICEHG DS dataset (Section 3.1), remains critical [51]. Limited datasets from single medical centers also restrict generalizability across diverse populations. Future work should prioritize larger, multi-regional datasets to enhance the clinical applicability and robustness of EHG-based models.

4.3 Rationale for classifier and channel selection

The proposed classifiers, RF, SVM, and LSTM were chosen for preterm labor prediction using the ICEHG DS dataset due to their suitability for small datasets and proven effectiveness in EHG analysis [9, 52]. The limited dataset size (126 deliveries) makes complex models like Transformers impractical, as they require large data to avoid overfitting. RF, SVM, and LSTM offer computational efficiency for home-based monitoring, unlike resource-intensive Transformers [23, 52]. The extracted features (Sh-En, LogEn) are compatible with RF and SVM for structured data and LSTM for sequential data, aligning with standard EHG studies [9]. These classifiers ensure reliability even without synthetic data (unlike ADASYN, etc.). Future work may explore larger datasets for advanced models.

Hyperparameter tuning was performed to ensure reproducibility using 10-fold stratified cross-validation on the ICEHG DS dataset (19 Cesarean, 81 induced, 26 induced-cesarean deliveries) in MATLAB R2024a. For Random Forest (RF), the number of trees and maximum depth were tuned via grid search in the Classification Learner app, achieving an F1-score of 98.89%. For Support Vector Machine (SVM), kernel type (linear, RBF, polynomial) and regularization parameter C were optimized automatically, yielding an F1-score of 99.21%. For Long Short-Term Memory (LSTM), the number of layers and units per layer were adjusted in the Neural Network Toolbox, resulting in an F1-score of 99.34%. These settings, optimized on real data independently of ADASYN (Section 4.2), align with EHG studies [9, 22].

As noted in the article [30], Channel S3, derived from

horizontally placed abdominal electrodes, performs better in separating preterm and term records ($p=1.1\times10^{5}$ for MF in B01 band). This is likely due to its high sensitivity to low-frequency signals (0.08-0.3 Hz, Fast Wave Low) associated with uterine contractions, while reducing maternal cardiac and respiratory noise (>1.0 Hz) [22]. We also used this channel in our study, and the results confirm the correctness of our choice.

4.4 Computational efficiency, real-time monitoring feasibility, and limitations

This section evaluates the computational efficiency and real-time applicability of the RF, SVM, and LSTM classifiers using the ICEHG DS dataset (1,448 frames per record). The feature extraction process, Sh-En (1.2 s), LogEn (0.56 s), and their combination (1.5 s per record) take approximately 0.39 to 1.04 ms per frame, which is well below the EHG sampling interval of 50 ms (20 Hz), enabling real-time data processing.

Table 6 summarizes the average training and inference times across 10-fold cross-validation, averaged over 10 independent runs using MATLAB's timeit function. The reported inference times are significantly lower than the EHG frame interval, supporting the feasibility of real-time monitoring using the proposed models. These results are consistent with prior EHG-based studies [9, 52], which typically report processing latencies between 10–100 μs per sample.

Table 6. Computational Efficiency Metrics for RF, SVM, and LSTM

Classifier	Training Time/Fold (s)	Inference Time (ms)
RF	17.5 ± 1.5	83.5 ± 0.3
SVM	70.4 ± 5.3	24.1 ± 0.2
LSTM	71.0 ± 4.6	28.9 ± 0.5

In terms of clinical deployment, these latency metrics suggest compatibility with portable fetal monitoring devices such as the Monica AN24 [11], which operate within similar real-time constraints. However, several deployment challenges remain, including potential signal noise in ambulatory environments, limited processing power on edge devices, and the relatively small size and diversity of the dataset, which may affect model generalizability. As part of future work, we aim to: further optimize model latency for embedded and low-power platforms, expand the dataset through multi-center collaborations to enhance robustness, and explore lightweight deep learning architectures that maintain accuracy while reducing computational demands.

5. CONCLUSION

This study presents a computationally efficient method for classifying delivery types (induced, cesarean, and induced-cesarean) using EHG signals as early as the 23rd week of pregnancy. By leveraging two simple yet sensitive features, Shannon Entropy and Logarithmic Energy extracted from a single EHG channel, our approach achieves high accuracy (99.34% F1-score) without requiring complex models. The use of data augmentation techniques, such as ADASYN, effectively addressed class imbalance, yielding robust performance despite data limitations. Beyond its technical merits, this method offers significant clinical potential by enabling early identification of delivery type risks, allowing clinicians to optimize labor induction strategies, reduce unnecessary cesarean sections, and mitigate maternal and neonatal complications. This predictive capability supports personalized obstetric care, potentially alleviating the global burden of preterm birth and associated adverse outcomes. The low computational complexity of our approach also makes it suitable for integration into portable EHG devices, facilitating real-time monitoring in clinical settings. However, for real-time deployment, further optimization may be necessary to reduce computational latency and ensure compatibility with wearable or portable hardware. Future work will focus on validating the method across diverse populations and exploring hardware-friendly architectures to enhance its practical utility in maternal healthcare.

REFERENCES

[1] World Health Organization. (2023). Preterm birth: Fact sheets. https://www.who.int/news-room/fact-sheets/detail/preterm-birth, accessed on Aug. 4, 2025.

[2] Perin, J., Mulick, A., Yeung, D., Villavicencio, F., Lopez, G., et al. (2022). Global, regional, and national causes of under-5 mortality in 2000–19: An updated systematic analysis with implications for the Sustainable Development Goals. The Lancet Child & Adolescent Health, 6(2): 106-115. https://doi.org/10.1016/S2352-4642(21)00311-4

[3] Balu, D.T. (2017). Cognitive deficits in prematurely born adults are associated with reduced basal forebrain integrity. Biological Psychiatry, 82(2): e15. https://doi.org/10.1016/j.biopsych.2017.04.004

[4] Ream, M.A., Lehwald, L. (2018). Neurologic consequences of preterm birth. Current Neurology and Neuroscience Reports, 18: 1-10. https://doi.org/10.1007/s11910-018-0862-2

[5] Buhimschi, C., Boyle, M.B., Garfield, R.E. (1997). Electrical activity of the human uterus during pregnancy as recorded from the abdominal surface. Obstetrics & Gynecology, 90(1): 102-111. https://doi.org/10.1016/S0029-7844(97)83837-9

[6] Verdenik, I., Pajntar, M., Leskošek, B. (2001). Uterine electrical activity as predictor of preterm birth in women with preterm contractions. European Journal of Obstetrics & Gynecology and Reproductive Biology, 95(2): 149-153. https://doi.org/10.1016/S0301-2115(00)00418-8

[7] Maner, W.L., Garfield, R.E., Maul, H., Olson, G., Saade, G. (2003). Predicting term and preterm delivery with transabdominal uterine electromyography. Obstetrics & Gynecology, 101(6): 1254-1260. https://doi.org/10.1016/S0029-7844(03)00341-7

[8] Marque, C.K., Terrien, J., Rihana, S., Germain, G. (2007). Preterm labour detection by use of a biophysical marker: The uterine electrical activity. BMC Pregnancy and Childbirth 7(1): 2876–2887. https://doi.org/10.1186/1471-2393-7-S1-S5

[9] Jager, F., Libenšek, S., Geršak, K. (2018). Characterization and automatic classification of preterm and term uterine records. PLoS One, 13(8): e0202125. https://doi.org/10.1371/journal.pone.0202125

[10] Garcia-Casado, J., Ye-Lin, Y., Prats-Boluda, G., Mas-Cabo, J., Alberola-Rubio, J., Perales, A. (2018).

Electrohysterography in the diagnosis of preterm birth: A review. Physiological Measurement, 39(2): 02TR01. https://doi.org/10.1088/1361-6579/aaad56

[11] Marque, C., Duchene, J.M., Leclercq, S., Panczer, G.S., Chaumont, J. (2007). Uterine EHG processing for obstetrical monitorng. IEEE Transactions on Biomedical Engineering, 12: 1182-1187. https://doi.org/10.1109/TBME.1986.325698

[12] Devedeux, D., Marque, C., Mansour, S., Germain, G., Duchêne, J. (1993). Uterine electromyography: A critical review. American Journal of Obstetrics and Gynecology, 169(6): 1636-1653. https://doi.org/10.1016/0002-9378(93)90456-S

[13] Lucovnik, M., Maner, W.L., Chambliss, L.R., Blumrick, R., Balducci, J., Novak-Antolic, Z., Garfield, R.E. (2011). Noninvasive uterine electromyography for prediction of preterm delivery. American Journal of Obstetrics and Gynecology, 204(3): 228-e1. https://doi.org/10.1016/j.ajog.2010.09.024

[14] Fele-Žorž, G., Kavšek, G., Novak-Antolič, Ž., Jager, F. (2008). A comparison of various linear and non-linear signal processing techniques to separate uterine EMG records of term and pre-term delivery groups. Medical & Biological Engineering & Computing, 46: 911-922. https://doi.org/10.1007/s11517-008-0350-y

[15] Richman, J.S., Moorman, J.R. (2000). Physiological time-series analysis using approximate entropy and sample entropy. American Journal of Physiology-Heart and Circulatory Physiology, 278(6): H2039-H2049. https://doi.org/10.1152/ajpheart.2000.278.6.H2039

[16] Hassan, M., Terrien, J., Marque, C., Karlsson, B. (2011). Comparison between approximate entropy, correntropy and time reversibility: Application to uterine electromyogram signals. Medical Engineering & Physics, 33(8): 980-986. https://doi.org/10.1016/j.medengphy.2011.03.010

[17] Lemancewicz, A., Borowska, M., Kuć, P., Jasińska, E., Laudański, P., Laudański, T., Oczeretko, E. (2016). Early diagnosis of threatened premature labor by electrohysterographic recordings–The use of digital signal processing. Biocybernetics and Biomedical Engineering, 36(1): 302-307. https://doi.org/10.1016/j.bbe.2015.11.005

[18] Ozbek, I.Y., Shamsi, H. (2015). Heart sound localization in respiratory sound based on a new computationally efficient entropy bound. IEEE Journal of Biomedical and Health Informatics, 21(1): 105-114. https://doi.org/10.1109/JBHI.2015.2491500

[19] Rostaghi, M., Azami, H. (2016). Dispersion entropy: A measure for time-series analysis. IEEE Signal Processing Letters, 23(5): 610-614. https://doi.org/10.1109/LSP.2016.2542881

[20] Manis, G., Aktaruzzaman, M.D., Sassi, R. (2017). Bubble entropy: An entropy almost free of parameters. IEEE Transactions on Biomedical Engineering, 64(11): 2711-2718. https://doi.org/10.1109/TBME.2017.2664105

[21] Nieto-del-Amor, F., Beskhani, R., Ye-Lin, Y., Garcia-Casado, J., Diaz-Martinez, A., et al. (2021). Assessment of dispersion and bubble entropy measures for enhancing preterm birth prediction based on electrohysterographic signals. Sensors, 21(18): 6071. https://doi.org/10.3390/s21186071

[22] Acharya, U.R., Sudarshan, V.K., Rong, S.Q., Tan, Z., Lim, C.M., et al. (2017). Automated detection of premature delivery using empirical mode and wavelet packet decomposition techniques with uterine electromyogram signals. Computers in Biology and Medicine, 85: 33-42. https://doi.org/10.1016/j.compbiomed.2017.04.013

[23] Mohammadi Far, S., Beiramvand, M., Shahbakhti, M., Augustyniak, P. (2022). Prediction of preterm delivery from unbalanced EHG database. Sensors, 22(4): 1507. https://doi.org/10.3390/s22041507

[24] Mas-Cabo, J., Prats-Boluda, G., Garcia-Casado, J., Alberola-Rubio, J., Monfort-Ortiz, R., et al. (2020). Electrohysterogram for ANN-based prediction of imminent labor in women with threatened preterm labor undergoing tocolytic therapy. Sensors, 20(9): 2681. https://doi.org/10.3390/s20092681

[25] Kaiser, J.F. (1990). On a simple algorithm to calculate the 'energy' of a signal. In International Conference on Acoustics, Speech, and Signal Processing, Albuquerque, NM, USA, pp. 381-384. https://doi.org/10.1109/ICASSP.1990.115702

[26] Kaiser, J.F. (1993). Some useful properties of Teager's energy operators. In 1993 IEEE International Conference on Acoustics, Speech, and Signal Processing, Minneapolis, MN, USA, pp. 149-152. https://doi.org/10.1109/ICASSP.1993.319457

[27] Fergus, P., Selvaraj, M., Chalmers, C. (2018). Machine learning ensemble modelling to classify caesarean section and vaginal delivery types using Cardiotocography traces. Computers in Biology and Medicine, 93: 7-16. https://doi.org/10.1016/j.compbiomed.2017.12.002

[28] Alberola-Rubio, J., Garcia-Casado, J., Prats-Boluda, G., Ye-Lin, Y., Desantes, D., Valero, J., Perales, A. (2017). Prediction of labor onset type: Spontaneous vs induced; role of electrohysterography? Computer Methods and Programs in Biomedicine, 144: 127-133. https://doi.org/10.1016/j.cmpb.2017.03.018

[29] Fele-Žorž, G., Kavšek, G., Novak-Antolič, Ž., Jager, F. (2008). A comparison of various linear and non-linear signal processing techniques to separate uterine EMG records of term and pre-term delivery groups. Medical & Biological Engineering & Computing, 46: 911-922. https://doi.org/10.1007/s11517-008-0350-y

[30] Pirnar, Ž., Jager, F., Geršak, K. (2022). Characterization and separation of preterm and term spontaneous, induced, and cesarean EHG records. Computers in Biology and Medicine, 151: 106238. https://doi.org/10.1016/j.compbiomed.2022.106238

[31] Mischi, M., Chen, C., Ignatenko, T., de Lau, H., Ding, B., Oei, S.G., Rabotti, C. (2017). Dedicated entropy measures for early assessment of pregnancy progression from single-channel electrohysterography. IEEE Transactions on Biomedical Engineering, 65(4): 875-884. https://doi.org/10.1109/TBME.2017.2723933

[32] Ahmed, M.U., Chanwimalueang, T., Thayyil, S., Mandic, D.P. (2016). A multivariate multiscale fuzzy entropy algorithm with application to uterine EMG complexity analysis. Entropy, 19(1): 2. https://doi.org/10.3390/e19010002

[33] Degbedzui, D.K., Yüksel, M.E. (2020). Accurate diagnosis of term–preterm births by spectral analysis of electrohysterography signals. Computers in Biology and Medicine, 119: 103677.

https://doi.org/10.1016/j.compbiomed.2020.103677
[34] Xu, J., Chen, Z., Zhang, J., Lu, Y., Yang, X., Pumir, A. (2021). Realistic preterm prediction based on optimized synthetic sampling of EHG signal. Computers in Biology and Medicine, 136: 104644. https://doi.org/10.1016/j.compbiomed.2021.104644
[35] Fergus, P., Cheung, P., Hussain, A., Al-Jumeily, D., Dobbins, C., Iram, S. (2013). Prediction of preterm deliveries from EHG signals using machine learning. PloS One, 8(10): e77154. https://doi.org/10.1371/journal.pone.0077154
[36] Hussain, A.J., Fergus, P., Al-Askar, H., Al-Jumeily, D., Jager, F. (2015). Dynamic neural network architecture inspired by the immune algorithm to predict preterm deliveries in pregnant women. Neurocomputing, 151: 963-974. https://doi.org/10.1016/j.neucom.2014.03.087
[37] Smrdel, A., Jager, F. (2015). Separating sets of term and pre-term uterine EMG records. Physiological Measurement, 36(2): 341. https://doi.org/10.1088/0967-3334/36/2/341
[38] Ren, P., Yao, S., Li, J., Valdes-Sosa, P.A., Kendrick, K.M. (2015). Improved prediction of preterm delivery using empirical mode decomposition analysis of uterine electromyography signals. PloS One, 10(7): e0132116. https://doi.org/10.1371/journal.pone.0132116
[39] Fergus, P., Idowu, I., Hussain, A., Dobbins, C. (2016). Advanced artificial neural network classification for detecting preterm births using EHG records. Neurocomputing, 188: 42-49. https://doi.org/10.1016/j.neucom.2015.01.107
[40] Chen, L., Xu, H. (2020). Deep neural network for semi-automatic classification of term and preterm uterine recordings. Artificial Intelligence in Medicine, 105: 101861. https://doi.org/10.1016/j.artmed.2020.101861
[41] Saleem, S., Saeed, A., Usman, S., Ferzund, J., Arshad, J., Mirza, J., Manzoor, T. (2020). Granger causal analysis of electrohysterographic and tocographic recordings for classification of term vs. preterm births. Biocybernetics and Biomedical Engineering, 40(1): 454-467. https://doi.org/10.1016/j.bbe.2020.01.007
[42] Peng, J., Hao, D., Yang, L., Du, M., Song, X., et al. (2020). Evaluation of electrohysterogram measured from different gestational weeks for recognizing preterm delivery: A preliminary study using random forest. Biocybernetics and Biomedical Engineering, 40(1): 352-362. https://doi.org/10.1016/j.bbe.2019.12.003
[43] Nieto-del-Amor, F., Prats-Boluda, G., Martinez-De-Juan, J.L., Diaz-Martinez, A., Monfort-Ortiz, R., Diago-Almela, V.J., Ye-Lin, Y. (2021). Optimized feature subset selection using genetic algorithm for preterm labor prediction based on electrohysterography. Sensors, 21(10): 3350. https://doi.org/10.3390/s21103350
[44] Nieto-del-Amor, F., Beskhani, R., Ye-Lin, Y., Garcia-Casado, J., Diaz-Martinez, A., et al. (2021). Assessment of dispersion and bubble entropy measures for enhancing preterm birth prediction based on electrohysterographic signals. Sensors, 21(18): 6071. https://doi.org/10.3390/s21186071
[45] Xu, J., Wang, M., Zhang, J., Chen, Z., Huang, W., Shen, G., Zhang, M. (2022). Network theory based EHG signal analysis and its application in preterm prediction. IEEE Journal of Biomedical and Health Informatics, 26(7): 2876-2887. https://doi.org/10.1109/JBHI.2022.3140427
[46] Mas-Cabo, J., Ye-Lin, Y., Garcia-Casado, J., Díaz-Martinez, A., Perales-Marin, A., et al. (2020). Robust characterization of the uterine myoelectrical activity in different obstetric scenarios. Entropy, 22(7): 743. https://doi.org/10.3390/e22070743
[47] Parra, C.B., Tendero, A.I., Ye-Lin, Y., Alberola-Rubio, J., Marin, A.P., Garcia-Casado, J., Prats-Boluda, G. (2018). Feasibility of labor induction success prediction based on uterine myoelectric activity spectral analysis. Biosignals, 4: 70-77. https://doi.org/10.5220/0006649400700077
[48] Benalcazar-Parra, C., Ye-Lin, Y., Garcia-Casado, J., Monfort-Ortiz, R., Alberola-Rubio, J., Perales, A., Prats-Boluda, G. (2019). Prediction of labor induction success from the uterine electrohysterogram. Journal of Sensors, 2019(1): 6916251. https://doi.org/10.1155/2019/6916251
[49] Fernández, A.D.R., Fernández, D.R., Sánchez, M.T.P. (2022). Prediction of the mode of delivery using artificial intelligence algorithms. Computer Methods and Programs in Biomedicine, 219: 106740. https://doi.org/10.1016/j.cmpb.2022.106740
[50] Diaz-Martinez, A., Mas-Cabo, J., Prats-Boluda, G., Garcia-Casado, J., Cardona-Urrego, K., et al. (2020). A comparative study of vaginal labor and caesarean section postpartum uterine myoelectrical activity. Sensors, 20(11): 3023. https://doi.org/10.3390/s20113023
[51] Jager, F. (2023). An open dataset with electrohysterogram records of pregnancies ending in induced and cesarean section delivery. Scientific Data, 10(1): 669. https://doi.org/10.1038/s41597-023-02581-6
[52] Mohammadi Far, S., Beiramvand, M., Shahbakhti, M., Augustyniak, P. (2023). Prediction of preterm labor from the electrohysterogram signals based on different gestational weeks. Sensors, 23(13): 5965. https://doi.org/10.3390/s23135965
[53] He, H., Bai, Y., Garcia, E.A., Li, S. (2008). ADASYN: Adaptive synthetic sampling approach for imbalanced learning. In 2008 IEEE International Joint Conference on Neural Networks (IEEE World Congress on Computational Intelligence), Hong Kong, pp. 1322-1328. https://doi.org/10.1109/IJCNN.2008.4633969